An indigenous echelle grating spectrograph for simultaneous trace elemental analysis by atomic emission spectroscopy

Dinesh V. Udupa, Sanjiva Kumar, Omana Narayanan, Padma B. Patil, S. Ajaykumar, R. Sampathkumar, K. Thankarajan and Naba K. Sahoo

Detailed optical design and construction of an indigenously developed echelle grating spectrograph for simultaneous spectrochemical analysis of up to 51 elements by optical emission spectroscopy are presented here. The spectrograph consists of two concave spherical mirrors for collimation and focusing, an echelle grating with groove frequency of 79 lines/mm, and a two-dimensional CCD detector for recording the spectral lines. Fused silica Littrow prism is used for sorting the different spectral orders of 60–120 in the spectrum. The instrument has a wavelength range 200–400 nm with a resolving power of 15,000. The reciprocal linear dispersion of the instrument is 0.353 nm/mm at a wavelength of 300 nm. Results of simultaneous spectrochemical analysis using the inductively coupled plasma source of excitation are also presented.

Echelle grating spectrographs have found applications as high-resolution instruments in astrophysics and astronomy mainly due to advantages such as high resolution with wavelength tunability, larger throughput, compactness in size and rugged design[1–3]. Laser-induced breakdown spectroscopy (LIBS)-based analytical techniques are often implemented with echelle spectrographs for taking due advantage of large-wavelength bandwidths offered by them[4–9]. Over the years, echelle spectrographs are being increasingly used for analytical applications using emission spectroscopy, Raman spectroscopy and for other spectroscopic investigations in laboratories and industry[10–17]. A charge coupled device (CCD)-based echelle grating spectrograph offers several advantages over the discreet polychromator type 'direct' reading instrument for simultaneous multi-element analysis. The chief advantage is the freedom of choosing analytical lines since data are recorded in a continuous spectrograph mode. Another advantage is the relative compact size of the instrument in comparison to photomultiplier tube (PMT)-based polychromators, whose size is constrained by the requirement of relatively large reciprocal linear wavelength dispersion. The simplicity of the detector electronics offered by a single CCD detector in comparison to multiple PMTs is another merit. The only de-merit as seen from a spectrochemical analytical viewpoint in a CCD-based instrument is the inability to adjust the relative sensitivities of the spectral lines if so required, as against PMT-based polychromators, where this is done by varying the PMT voltages.

We describe here the optical design, construction and performance of an echelle grating spectrograph for simultaneous spectrochemical analysis of elements by atomic emission spectrometry. The spectral range of the instrument is 200–400 nm with a resolution of 0.02 nm at 300 nm.

Optical design

A schematic optical diagram of the echelle spectrograph is shown in Figure 1. The optical design of the spectrograph is based on Czerny–Turner configuration with the echelle grating as the main dispersing element. The main feature in an echelle grating is the large blaze angle on the grooves designed for usage at high orders of interference for enhancing spectral resolution and dispersion. Consequent to the high order of interference, there is an overlap of a large number of neighbouring orders of close wavelengths in the diffracted light. A second dispersion by means of a fused silica Littrow prism is used, serving as an order sorter by separating the overlapping orders. In practice the prism is used as the first dispersing element (Figure 1). Light from an entrance slit is collimated by a concave spherical mirror M_1. The collimated light is dispersed by a fused silica Littrow prism P and then by an echelle grating G. The dispersion direction of the echelle grating is perpendicular to the dispersion direction of the prism producing a two-dimensionally dispersed light. The dispersed light is focused on a 2D CCD detector by another concave spherical mirror M_2 for recording the spectrum.

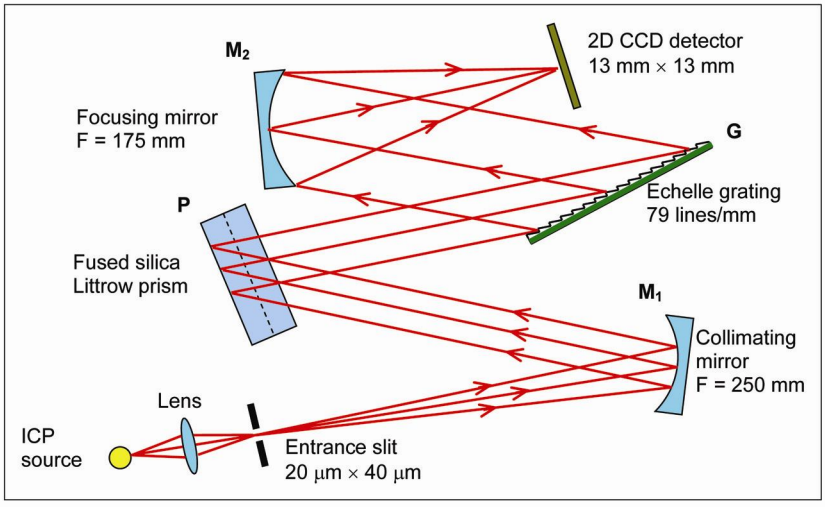

Figure 1. Optical layout of echelle spectrograph.

The important parameters to be fixed in the optical design of the spectrometer are the angle of incidence on the echelle grating, the focal lengths of the two mirrors M_1 and M_2, and the apex angle of the Littrow prism. The angle of incidence on the echelle grating must be close to the blaze angle for having higher diffraction efficiency.

Grating dispersion

The diffraction of the grating is described by the well-known equation

$$d(\sin\alpha + \sin\beta) = m\lambda_m, \quad (1)$$

where d is the groove spacing of the echelle grating, α the angle of incidence, β the angle of diffraction, m the order of interference and λ_m is the wavelength.

If θ_B is the grating blaze angle, then for high diffraction efficiency we must have

$$\alpha = \theta_B + \delta, \quad (2)$$

and

$$\beta = \theta_B - \delta, \quad (3)$$

where δ is a small constant angle, which is set to 7° in our case purely from geometrical considerations in the optical arrangement.

For a design with the wavelength range 200–400 nm, we get the angle of incidence $\alpha = 81°$ and the angle of diffraction $\beta = 67°$ for the central wavelength of 300 nm from eq. (3). This gives the order $m \approx 80$ for 300 nm from eq. (1). It follows from eq. (1) that all the wavelengths λ_k diffracted in spectral order k, and satisfying the condition

$$k \cdot \lambda_k = m \cdot \lambda_m, \quad (4)$$

emerge from the grating in the same direction and hence will overlap. An order-sorter having a low dispersion in the perpendicular direction is thus essential for separating overlapping spectral orders. In order to record the complete spectral range on the detector plane with minimum overlap, we calculate the angular spread $\Delta\beta$ in the grating diffraction. Rewriting eq. (1) as

$$d\{\sin(\theta_B + \delta) + \sin(\theta_B - \delta)\} = \Psi_C, \quad (5)$$

where $\Psi_C = m\lambda_m$ for the central wavelength, we see that the maximum and minimum orders diffracted at the same angle are related to maximum and minimum wavelength as

$$m_{max} = \frac{\Psi_C}{\lambda_{min}} \quad \text{and} \quad m_{min} = \frac{\Psi_C}{\lambda_{max}}. \quad (6)$$

We define the extreme limits in the range of Ψ as Ψ_{max} and Ψ_{min} corresponding to the angular spread ($\Delta\beta$) in the dispersed light along the grating dispersion plane. The values of Ψ_{max} and Ψ_{min} must be such that all wavelengths in the range must be covered with minimum overlap or repetition. This is possible if we have the wavelengths corresponding to Ψ_{min} for all orders to be less than or equal to the wavelengths corresponding to Ψ_{max} for the next consecutive order. Since wavelength dispersion is largest for the highest wavelength, we have the condition

$$\frac{\Psi_{max}}{(m_{min}+1)} = \frac{\Psi_{min}}{m_{min}}. \quad (7)$$

To the first approximation, if we assume a nearly linear dispersion we have

$$\Psi_{max} + \Psi_{min} = 2\Psi_C. \quad (8)$$

The angular diffraction range $\Delta\beta$ can be written down from eq. (1) as

$$\Delta\beta = \frac{\Delta\Psi}{d\cos\beta}. \quad (9)$$

The echelle grating in our instrument has the following specifications: (i) Groove density $(1/d) = 79$ lines/mm. (ii) Blaze angle $(\theta_B) = 74°$. (iii) Rulings: aluminium-coated with 120 mm × 254 mm size.

Substituting the parameters in eq. (5), we get $\Psi_C = 24{,}154.3$ nm and from eq. (6) we get $m_{max} = 120$ and $m_{min} = 60$. The values $\Psi_{max} = 24{,}353.9$ nm and $\Psi_{min} = 23{,}954.7$ nm are obtained by solving eqs (7) and (8). The corresponding diffraction angle range $\Delta\beta$ is 4.625°.

Prism dispersion

The wavelength range incident on the detector plane is decided by the choice of the dispersion due to the prism. The parameters of the prism are chosen so as to cover a wavelength range 200–400 nm in the prism dispersion plane. Since the dispersed light from both the prism and the grating is focused by the common focusing mirror M_2 on the detector plane, the maximum angular spread of the light dispersed by the prism covering the full spectral range must be equal to the grating diffraction angle range ($\Delta\beta$). The angle of incidence and the apex angle of the Littrow prism corresponding to this dispersion are calculated by the equations for prism dispersion.

For the central wavelength we have the condition (Figure 2)

$$\mu_C \sin A = \sin i, \quad (10)$$

where i is the angle of incidence, A the prism apex angle and μ_C is the refractive index for the central wavelength λ_C. For the extreme wavelengths the angle of emergence e is given by

$$\sin e = \mu_\lambda \sin(2A - r), \quad (11)$$

where μ_λ is the refractive index for wavelength λ and r is the refraction angle given by

$$\sin r = \frac{\sin i}{\mu_\lambda}. \quad (12)$$

For fused silica glass used in the prism, we have $\mu_\lambda = 1.55051$ for $\lambda = 200$ nm, $\mu_\lambda = 1.46962$ for $\lambda = 400$ nm and $\mu_C = 1.48719$ for $\lambda_C = 300$ nm. Using these values in eqs (10)–(12), and setting the range of emergence angle Δe between extreme wavelengths as 4.625°, we get the values $i = 36.20°$ and $A = 23.4°$.

Mirrors

Mirrors M_1 and M_2 are spherical mirrors used in off-axis. The off-axis angles of the mirrors are kept minimum possible

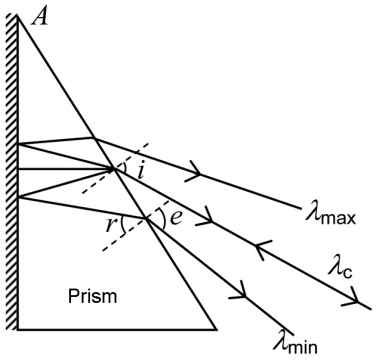

Figure 2. Schematic of dispersion in Littrow prism.

for accommodating the physical sizes of the components in the layout. The distance of the image plane l_2 from the mirror M_2 for imaging the dispersed light on the CCD detector of size D is calculated using the following equation

$$l_2 = \frac{D}{2\tan\left(\frac{\Delta\beta}{2}\right)}. \quad (13)$$

For a detector size of 13.3 mm × 13.3 mm, l_2 = 165 mm. Setting l_2 as the tangential focal plane of M_2, the radius of curvature R is calculated using the relation for the tangential focus

$$R = \frac{2l_2}{\cos\phi}, \quad (14)$$

where ϕ is the off-axis angle.

For $\phi = 20°$ in the design, R = 350 mm, making f_2 = 175 mm.

The focal length of the collecting mirror M_1 is arrived at by practical considerations and magnification requirements. For a practical entrance slit of 20 μm width and 40 μm height, the focal length f_1 of mirror M_1 is chosen to be 250 mm for de-magnifying the slit image on 13 μm pixel size. The size of the CCD used is 13.3 mm × 13.3 mm with 1024 × 1024 pixels of size 13 μm × 13 μm.

The grating wavelength dispersion is given by

$$\frac{\partial\beta}{\partial\lambda} = \frac{m}{d\cos\beta}. \quad (15)$$

The reciprocal linear grating dispersion on the image plane is

$$\frac{\partial\lambda}{\partial x} = \frac{d\cos\beta}{m f_2}. \quad (16)$$

Substituting the values $\partial\lambda/\partial x$ =0.353 nm/mm for 300 nm (80 order), this corresponds to 0.00459 nm per pixel on the CCD plane. Considering minimum separation of three pixels for resolution between closely spaced lines, the theoretical limit for resolution is 0.0138 nm at a wavelength of 300 nm. Similarly, the theoretical limits of resolution are 0.0092 and 0.0183 nm for 200 and 400 nm respectively, corresponding to theoretical limit for the resolving power of about 21,000. Table 1 summarizes the design parameters of the echelle spectrograph.

Optical aberrations

The chief optical aberrations affecting the spectral image quality and resolution are spherical aberration, astigmatism and coma. A mirror-based optical design ensures the elimination of chromatic aberration in this system. Since the total field covered by mirror M_2 is within 4.625° (±2.312°) for an off-axis angle of 20°, the variations in spot size due to coma across the field are small. This results in a near-constant resolution in the working range. While spherical aberration and coma are reduced using larger f number (f/8), the effects of astigmatism are minimized using a rectangular aperture on the mirror M_1. The width of the aperture is kept small (5 mm) compared to the length (25 mm), thereby limiting the sagittal rays so that the length of the astigmatic image on the image plane is less than inter-order spacing. The overall smaller apertures resulting from the above design can be afforded in this instrument considering the high intensity of light source used for illumination and a highly sensitive detector. It may also be mentioned here that the precision and accuracy of measurements for analytical applications are dependent on source stability and standards accuracy, since the measurements during analysis are of the peak intensities of spectral lines and are calibrated against standards. Optical aberrations in this instrument thus affect the overall lower limit of detection in spectrochemical analysis.

Table 1. Design parameters of echelle spectrograph

Wavelength range: 200–400 nm
Resolution: 0.02 nm at 300 nm
Entrance slit: 20 μm (width) × 40 μm (height)
Collimating mirror: concave spherical, aluminium-coated
Focal length: 250 mm
Off-axis angle: 7°
Focusing mirror: concave spherical, aluminium-coated
Focal length: 175 mm
Off-axis angle: 20°
Order sorter: fused silica Litttrow prism, aluminium-coated
Prism apex angle: 23°24′
Grating: echelle grating, aluminium-coated
Rulings: 79 lines/mm
Blaze angle: 74°
Angle of incidence on grating: 81°
Angle of diffraction: 67° for 300 nm
Detector: Peltier cooled two-dimensional CCD detector
Area: 13.3 mm × 13.3 mm
Pixel size: 13 μm × 13 μm
Elements: 1024 × 1024

Assembly, wavelength calibration and testing

The mechanical mounts of all the components were designed to hold them rigidly in the optical configuration on a 12 mm thick steel base plate. The collimation and focusing of the mirrors M_1 and M_2 were aligned and tested using Murty's shear plate interferometer[18,19] and a He–Ne laser. The initial angular setting of the echelle grating was adjusted by observing 38th order of diffracted light of 632.8 nm of He–Ne laser beam, which can be identified by counting the diffracted beams starting from the zero order. The crucial aspect in the wavelength calibration is the correct identification of the order of interference along with the wavelength at a given pixel position on the detector. The initial calibration is by assignments of the prominent spectral lines emitted by a mercury discharge lamp kept near the entrance slit. The spectral images were also used for the precise setting of the echelle grating, prism and the detector positions so as to cover the designed spectral range with a best spectral sharpness on the detector plane. Figure 3 shows the spectra of mercury recorded on the detector. The resolution of the instrument has been tested by recording two closely spaced spectral lines emitted by a beryllium hollow cathode lamp. Figure 4 shows the spectral image of the emission lines (249.473 and 249.456 nm) separated by 0.017 nm recorded using beryllium hollow cathode lamp as a source with an entrance slit size of 20 μm × 40 μm.

A more precise wavelength calibration was done by recording the spectrum of various hollow cathode lamps of 40 different elements and assigning the pixel positions for prominent spectral lines. A database of 4–5 analytical lines listing wavelength and the corresponding pixel positions for these elements is created for application in analysis.

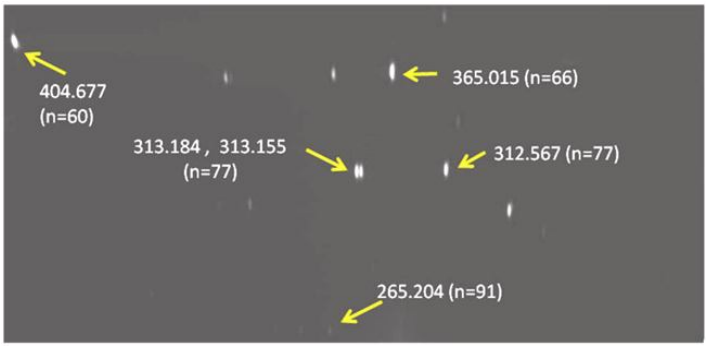

Figure 3. Mercury spectrum of a discharge lamp recorded using the spectrograph. This enlarged portion of the CCD image shows 13 mercury lines between 265.204 nm (91 order) and 404.677 nm (60 order) and was recorded for the optical alignment of the echelle spectrometer.

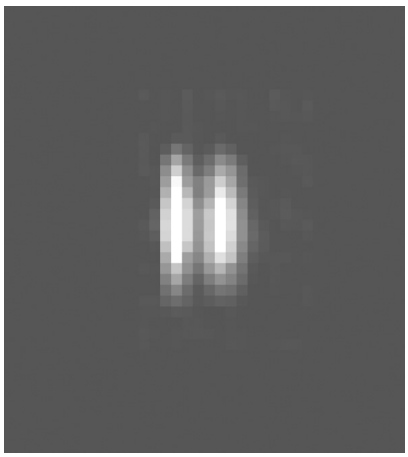

Figure 4. An enlarged section of the beryllium spectrum showing the resolved image of emission lines (249.473 and 249.456 nm) separated by 0.017 nm. This image was recorded by the instrument using beryllium hollow cathode lamp as a source.

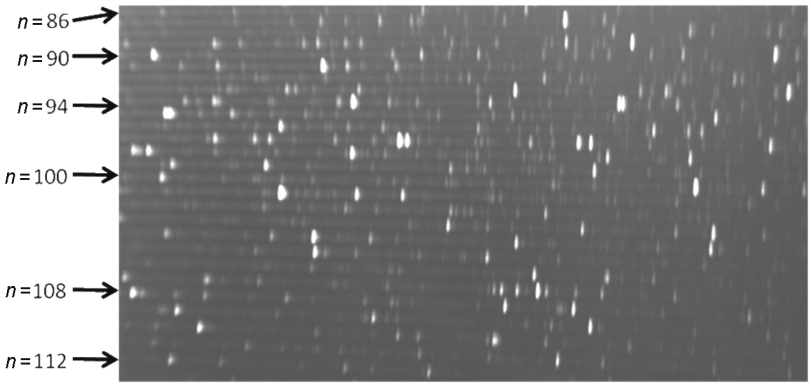

Figure 5. Spectra of the element tungsten in the 215–280 nm region (86–112 orders) recorded by introducing a 500 μg/ml tungsten aqueous solution in the inductively coupled plasma (ICP) flame. The contrast of the image has been enhanced to reveal the background emission of the ICP flame.

Data acquisition and analysis

The control, data acquisition and analysis are done by a personal computer interfaced to the CCD detector. A LabVIEW-based Virtual Instrument (VI) program has been written to perform spectrochemical analysis. The program has various menus that are available to the user to carry out the analysis. The Modify menu lets the user to set parameters that are common to all the impurities like the integration time, number of standards and type of standard. A menu in the program enables the user to set the temperature of the CCD detector from –40°C to 20°C. A menu item in the program helps the user to choose a new set of tabulated analytical conditions or continue with an old existing one with any changes if needed. The analysis menu provides the user with options to perform blank subtraction, background correction and impurity element estimation. The program runs the blank and standards as set in the table of analytical conditions, acquires the data from the CCD detector and stores the data into a file. The software gives the option to re-run a standard or a sample at every stage of the analysis. The data are then processed according to the set modes of analysis and the net counts are calculated. At this stage also the user is provided with a facility to reject bad data either cycle-wise or element-wise. The program generates a linear fit of the concentration versus counts data and plots the calibration curve for all the elements. Subsequently the program acquires counts from sample runs and estimates the sample concentration using the value of the slope and intercept of the calibration curve of all the elements.

Spectrochemical analysis and results

The spectrograph was aligned to an inductively coupled plasma (ICP) source having 1 kW radio frequency (RF) power with 27.12 MHz frequency for simultaneous spectrochemical analysis of elements. Light from the argon plasma in ICP torch is focused on the entrance slit by means of a fused silica lens. Best optical alignment between the analytical zone in the plasma flame and the spectrometer was ensured by maximizing signal to background ratio of boron line

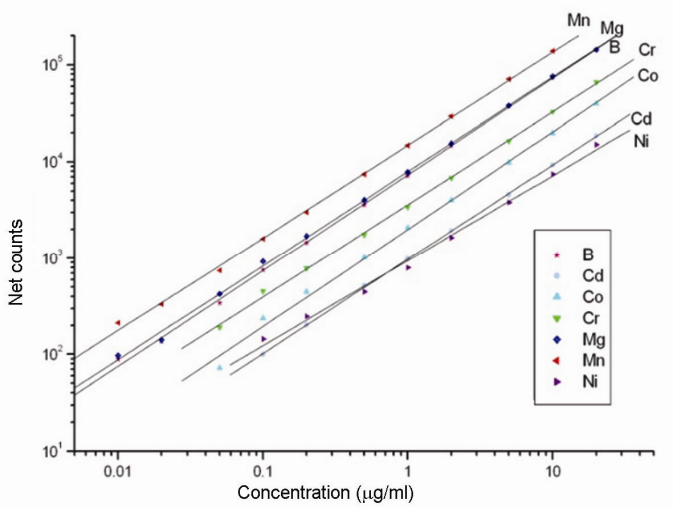

Figure 6. Calibration plot for the simultaneous analysis of seven elements. The concentration range is 0.01–20 μg/ml.

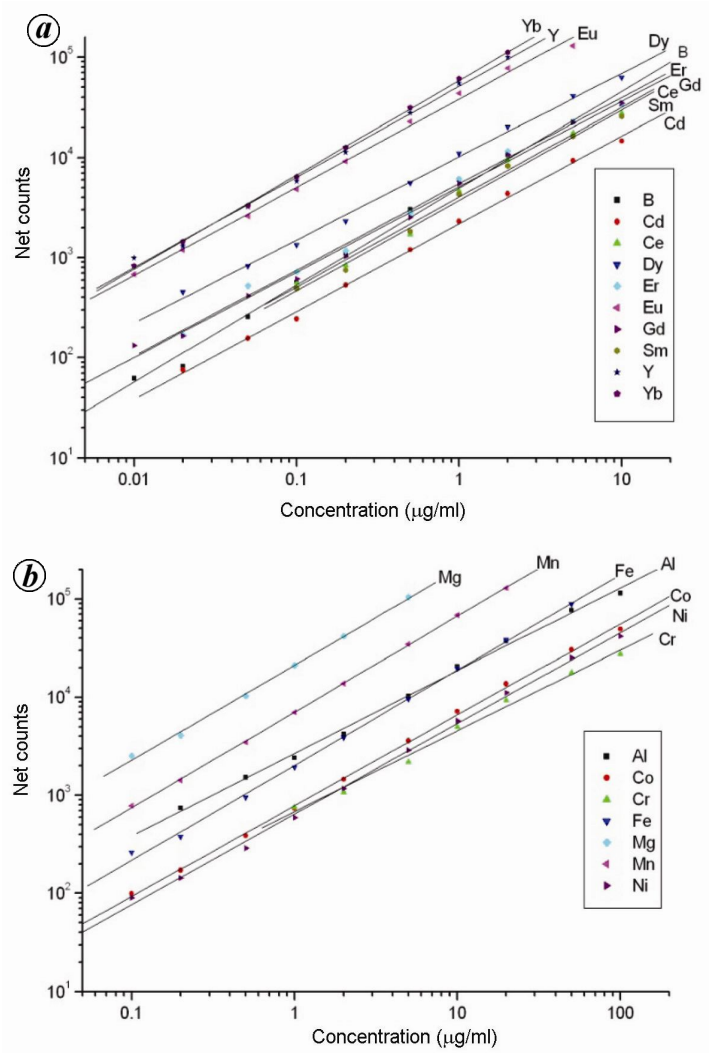

Figure 7. ***a***, Calibration plot for the simultaneous analysis of ten elements in the set of 17 elements. The concentration range is 0.01–10 μg/ml. ***b***, Calibration plot for the simultaneous analysis of seven elements in the set of 17 elements. The concentration range is 0.1–100 μg/ml.

(249.773 nm) recorded using 5 μg/ml boron aqueous standard. Figure 5 shows a portion of spectral image of tungsten emission lines recorded by introducing a 500 μg/ml tungsten aqueous solution in the ICP flame. The instrument was utilized for simultaneous analysis of seven most commonly assayed elements in uranium analysis, namely B, Cd, Co, Cr, Mg, Mn and Ni. For this purpose, initially stock solutions of concentration 1 mg/ml of each of these impurity element were prepared by dissolving metal or oxides (Spec-pure grade, Johnson Matthey Chemicals, UK) in electronic-grade concentrated or dilute nitric acid and making up the required volume by pure distilled de-ionized water. Using above stock solution, a composite master standard of 100 μg/ml was prepared, which was subsequently diluted to finally get a set of standards in the concentration range 0.01–10.0 μg/ml for the seven elements. Figure 6 shows the calibration plots of net counts (intensity) versus concentration of the seven elements in simultaneous analysis. Table 2 lists the corresponding determination limits for these seven elements.

In another experiment, a new set of aqueous standards containing 17 elements – Al, B, Cd, Co, Cr, Fe, Mg, Mn, Ni, Ce, Dy, Er, Eu, Gd, Sm, Y and Yb was prepared by making two sets of standards in the concentration range 0.01–10.0 μg/ml (for B, Cd, Ce, Gd, Er, Eu, Gd, Sm, Y and Yb) and 0.1–100 μg/ml (for Al, Co, Cr, Fe, Mg, Mn and Ni). Figure 7 *a* and *b* shows the calibration plots of net counts (intensity) versus concentration of the 17 elements in

Table 2. Lower determination limits in seven element analysis

Element	Concentration (μg/ml)
B, Mg, Mn	0.01
Cr	0.05
Cd, Co, Ni	0.1

Table 3. Lower determination limits in seventeen element analysis

Element	Concentration (μg/ml)
Eu, Y, Yb	0.01
B, Cd, Ce, Dy, Er, Gd	0.02
Mn, Mg, Fe, Sm	0.1
Al, Co, Ni	0.2
Cr	1.0

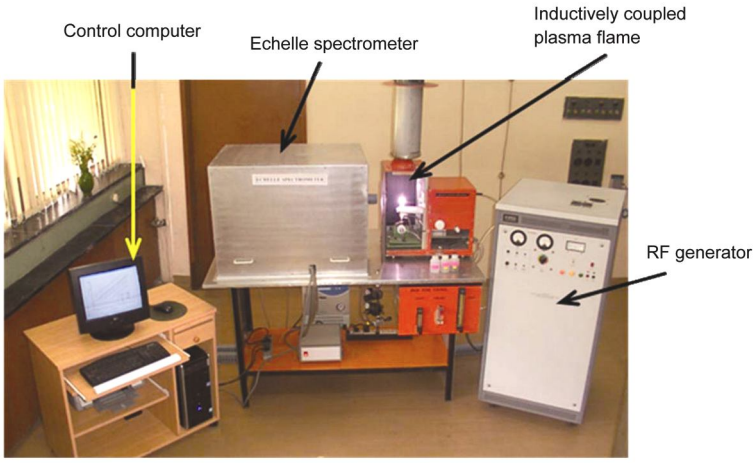

Figure 8. Photograph of the analytical system.

simultaneous analysis. Table 3 lists the corresponding determination limits for these 17 elements. Figure 8 shows a photograph of the analytical system.

Conclusions

An echelle grating spectrograph has been designed and constructed for simultaneous spectrochemical analysis of elements by optical emission spectroscopy. The instrument consists of an echelle grating as the main dispersion element and a cross-dispersing fused silica Littrow prism producing a two-dimensional spectrum on a 2D CCD detector. The instrument has been designed for a wavelength range 200–400 nm with a practical resolving power of 15,000. Various aspects relating to the optical design, assembly, alignment and calibration of the spectrograph have been presented. The spectrograph has been utilized for simultaneous analysis of 17 elements in aqueous medium using ICP excitation source.

1. Chakrabarti, S., Jokiaho, O.-P., Baumgardner, J., Cook, T., Martel, J. and Marina, *Opt. Eng.*, 2012, **51**(1), 013003.
2. Nevejans, D. *et al.*, *Appl. Opt.*, 2006, **45**(21), 5191–5206.
3. Panchuk, V. E., Klochkova, V. G., Yushkin, M. V. and Naidenov, I. D., *J. Opt. Technol.*, 2009, **76**(2), 87–97.
4. Unnikrishnan, V. K., Nayak, R., Aithal, K., Kartha, V. B., Santhosh, C., Gupta, G. P. and Suri, B. M., *Anal. Methods*, 2013, **5**, 1294–1300.
5. Hosseinimakarem, Z. and Tavassoli, S. H., *J. Biomed. Opt.*, 2011, **16**(5), 057002.
6. Stehrer, T. *et al.*, *J. Anal. At. Spectrom.*, 2009, **24**, 973–978.
7. Hamilton, S., Al-Wazzan, R., Hanvey, A., Varagnat, A. and Devlin, S., *J. Anal. At. Spectrom.*, 2004, **19**, 479–482.
8. Fichet, P., Menut, D., Brennetot, R., Vors, E. and Rivoallan, A., *Appl. Opt.*, 2003, **42**(30), 6029–6035.
9. Sabsabi, M., Detalle, V., Harith, M. A., Tawfik, W. and Imam, H., *Appl. Opt.*, 2003, **42**(30), 6094–6098.
10. Bruce True, J., Williams, R. H. and Bonner Denton, M., *Appl. Spectrosc.*, 1999, **53**(9), 1102–1110.
11. Becker-Ross, H., Florek, S., Franken, H., Radziuk, B. and Zeiher, M., *J. Anal. At. Spectrom.*, 2000, **15**, 851–861.
12. Florek, S. and Becker-Ross, H., *J. Anal. At. Spectrom.*, 1995, **10**, 145–147.
13. Spitsberg, A. T., Stephens, J. S., Deelo, M. and Hodges, C. E., *Appl. Spectrosc.*, 1999, **53**(11), 1472–1482.
14. Bye, C. A. and Scheeline, A., *Appl. Spectrosc.*, 1993, **47**(12), 2031–2035.
15. Scheeline, A., Bye, C. A., Miller, D. L., Rynders, S. W. and Calvin Owen Jr, R., *Appl. Spectrosc.*, 1991, **45**(3), 334–346.
16. Pelletier, M. J., *Appl. Spectrosc.*, 1990, **44**(10), 1699–1705.
17. Bilhorn, R. B. and Denton, M. B., *Appl. Spectrosc.*, 1989, **43**(1), 1–11.
18. Murty, M. V. R. K., *Appl. Opt.*, 1964, **3**, 531–534.
19. Shukla, R. P. and Malacara, D., *Opt. Lasers Eng.*, 1997, **26**, 1–42.

ACKNOWLEDGEMENTS. We thank Dr S. C. Sabharwal (Ex-Head, Spectroscopy Division, BARC, Mumbai) for support, encouragement and keen interest in this work. We also thank J. Thulasidoss and Kishore Thapa (Optics Workshop, BARC) for technical support in optical components fabrication; and Vijay Mhatre, R. S. Saroj, Hemant Koli and Sunil Kawade (Mechanical Workshop, BARC) for providing mechanical fabrication support during the construction and development stages of the spectrograph.

Received 30 January 2014; revised accepted 2 April 2014

Dinesh V. Udupa, Sanjiva Kumar, Omana Narayanan, Padma B. Patil, S. Ajaykumar, R. Sampathkumar, K. Thankarajan and Naba K. Sahoo are in the Atomic and Molecular Physics Division, Bhabha Atomic Research Centre, Mumbai 400 085, India.*
**e-mail: dudupa@barc.gov.in*